

Non-inductive current start-up and ramp-up by X-wave ECCD in fusion tokamaks

Takashi Maekawa, Masaki Uchida and Hitoshi Tanaka

Graduate School of Energy Science, Kyoto University, Kyoto, Japan

1. Introduction

In fusion tokamaks saving the flux swing during the current start-up and ramp-up phase is effective to prolong the burning duration, during which a very low loop-voltage is sufficient to maintain the toroidal current. Among various methods for saving, effective use of electron cyclotron heating and current drive (ECH/ECCD) power is important since the ECH/ECCD system would be already fabricated in fusion tokamaks to keep the burning phase stable via profile control. While Ordinary (O) waves at fundamental resonance frequency are supposed to be employed for control of the burning plasmas, extraordinary (X) waves are more useful than the O waves in low temperature and low density start-up plasmas [1]. Here X-waves are shown to be also useful in current ramp-up plasmas for an ITER case. It is also shown that a flux swing of about 10 volt seconds can be saved by 10 MW X-wave ECCD at initial current ramp up stage up to 1MA using a simple model for plasma current loop.

2. Performance of X-wave ECCD

The dispersion relations and wave polarizations were analysed based on the relativistic formula described in [2]. Current drive efficiencies in the toroidal geometry were estimated by assuming $Z_{\text{eff}}=2$ based on the quasi-linear theory and using the Green's function technique described in [3]. Figure 1 shows ray trajectories of X- and O-waves injected horizontally from various injection points at the low field side and the current drive efficiency as a function of Z coordinate at the injection point.

Generally, right hand circular component of wave polarization of the X-wave is quite large [1]. Therefore, the spatial damping rate quickly increases once the wave approaches toward the ECR layer and the fundamental EC resonance arises in the electron momentum space. The wave is damped away in a short distance of 0.2 m as shown in Figure 1(a). On the contrary, right hand circular component of the O-wave is negligibly small. While its spatial damping begins at the same location as the X-wave case, the damping rate is much weaker

than the X-wave rate and the wave is slowly damped with proceeding a long distance of ~ 1 m. Thus, locality of X-wave deposition is much higher than that of O-wave deposition. In addition, the farther the deposition location shifts to the lower field side from the ECR layer, the faster the resonance velocity becomes to the parallel direction apart from the trapped electron area, and the higher the current drive efficiency becomes. Right-hand circular polarization character of X-waves realizes a strong damping, which brings about a power deposition far from the ECR layer to the weak field side, resulting in an efficient current drive compared with the O-wave case.

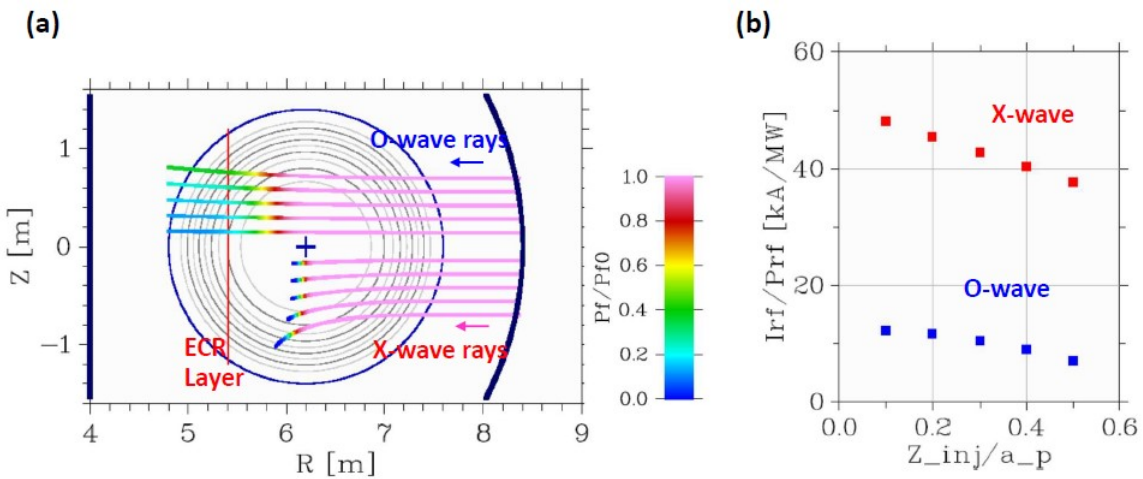


Figure 1 (a) Ray trajectories of X- and O-waves injected horizontally from $Z_{inj}/a_p=0.1$ to 0.5. Rainbow colours shows the power flux normalized to the injected value P_{f0} . Here, $a_p=1.4$ m is the plasma radius, $B_t=5.3$ T and $N_{\parallel}=0.6$ at $R=6.2$ m, frequency=170 GHz. Grey circles are contour plots for the temperature and density, decreasing by 10% step from the peak value of $T_{e0}=2.5$ keV and $n_{e0}=2.0 \times 10^{19} \text{ m}^{-3}$. (b) Current drive efficiency as a function of Z_{inj}/a_p .

Heating locality and current drive efficiency of X-wave and O-wave ECH/ECCD from the lower field side were numerically investigated for tokamak plasmas in the range of the electron temperature $T_{e0}=0.3$ to 22.5 keV and the density $n_{e0}=1.0$ to $3 \times 10^{19} \text{ m}^{-3}$, corresponding to the plasmas in the current start-up and ramp-up phases in fusion tokamaks. Performance of X-waves is better than that of O-waves up to $T_{e0}=15$ keV, over which O-wave performance still improves with T_{e0} , while X-wave performance deteriorates with T_{e0} due to the absorption via second harmonic resonance before the waves penetrate into the fundamental absorption area at the plasma core as shown in Figure 2.

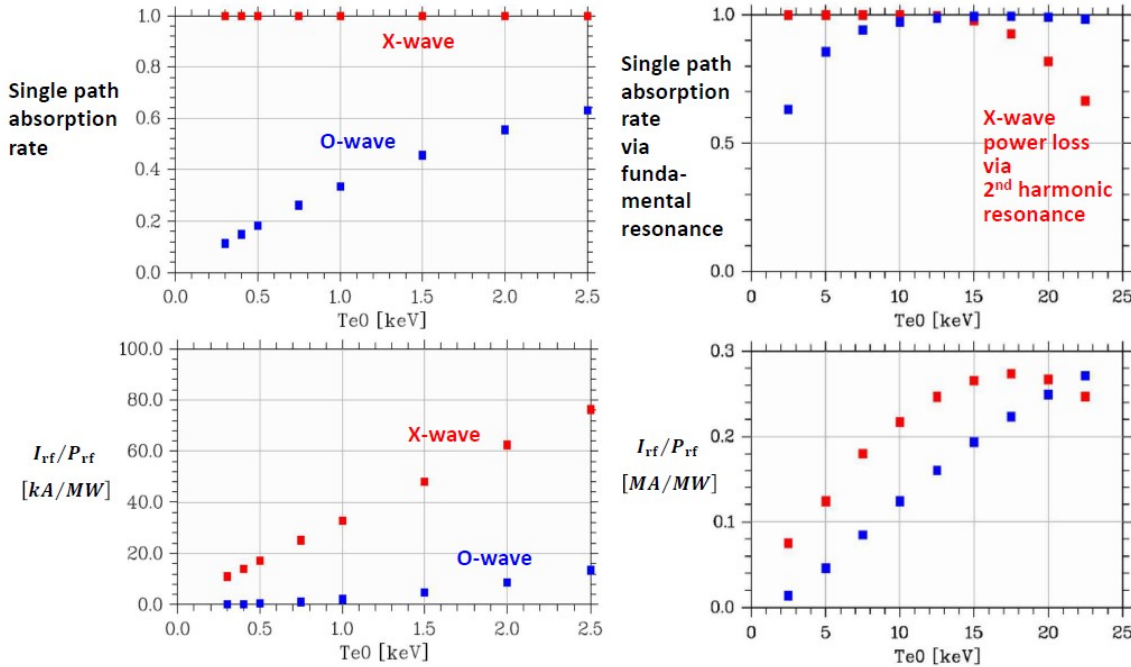


Figure 2 Single path absorption rate and current drive efficiency as functions of Te_0 for the same situation in Figure 1(a) except for $n_{e0}=1.0 \times 10^{19} m^{-3}$ and $Z_{inj}/a_p=0.25$. Roughly speaking, current drive efficiency I_{rf}/P_{rf} is inversely proportional to n_{e0} except for the O-wave cases of poor single path absorption rate.

3. Non inductive current ramp up using X-wave ECCD

As the Te increases into keV range, plasma conductivity becomes very high and the return current driven by the self-induction of EC driven current would hamper the current ramp-up. Here we study the current ramp-up for an ITER case using a current circuit model for the ECCD driven current and the return current. The circuit equation is coupled with the ECCD efficiency equation adjusted for X-wave ECCD described above [4] and the ITERL-97P energy confinement scaling [5].

The circuit equation is as follows;

$$V = I_E R_E = -d \Psi / dt \text{ with } \Psi = L_p I_p + L_{Bv} I_{Bv} \text{ and } I_p = I_{rf} + I_E. \quad (1)$$

Here, I_{rf} and I_E are the rf-driven non-inductive current and the return current, respectively. I_{Bv} is the coil current for the external vertical field Bv . L_{Bv} is estimated using the Shafranov formula for the equilibrium field Bv for a large aspect ratio torus having a circular cross section. Figure 3 shows a result in which the toroidal current is ramped up from $I_p=100$ kA to 1 MA during 200 sec by injection of $P_{rf} \sim 9$ MW. Electron temperature and plasma radius are assumed to change with I_p as $T_e \propto I_p^{0.66}$ and $a_p \propto I_p^{0.22}$.

$I_{rf}(t)$ is the driving term and all other quantities including P_{rf} , V , I_E etc are given as functions of time from equation (1) and shown in Figure 3 (a) and (b). The parameters are adjusted so that the energy confinement time U_p/Prf approximately coincides with the L-mode scaling as shown in Figure 3(c). The radial location of power deposition R_{abs} shifts to the lower field side as I_p ramps up and T_e increases as shown in Figure 3(d). Time integration of V in Figure 3(a) gives saving of the inductive consumption of ~ 10 Vs in addition to the resistive consumption.

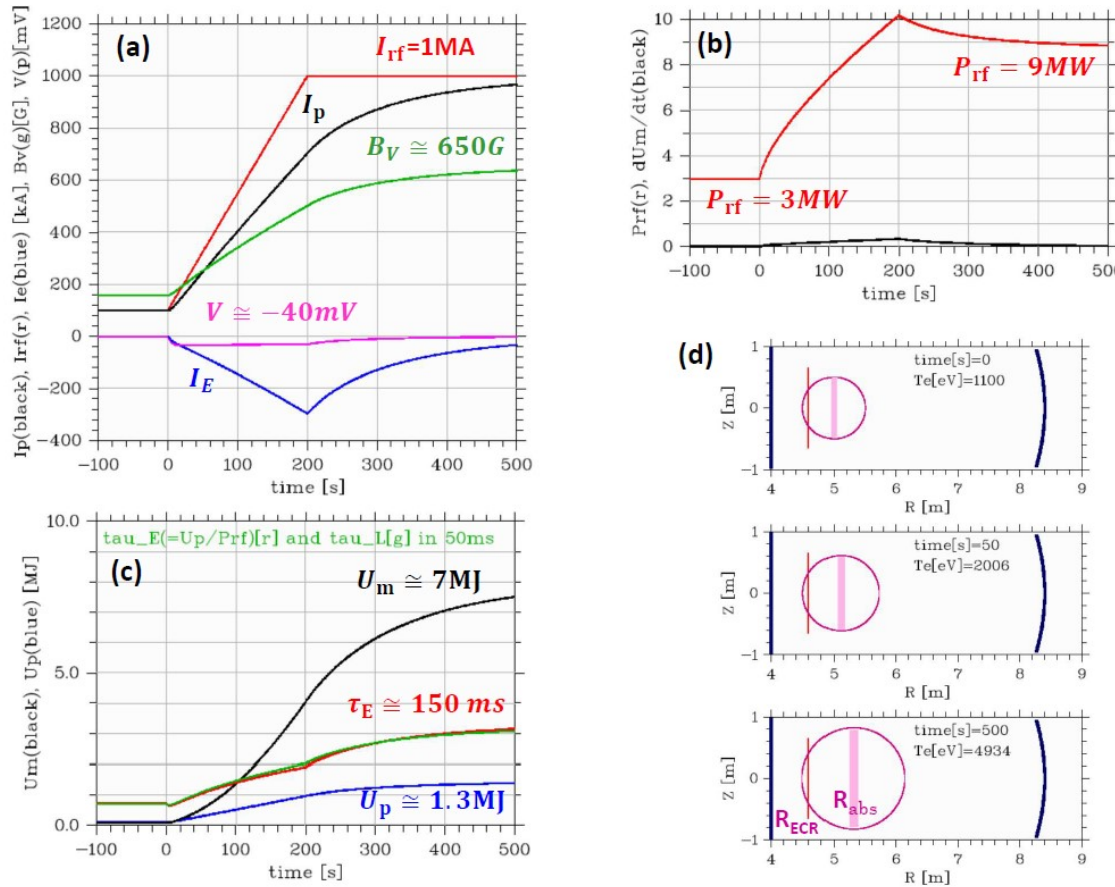


Figure 3 Time evolutions of (a) various currents etc., (b) rf power, (c) energy confinement time and plasma and magnetic energy of current loop and (d) plasma cross section.

Frequency=200 GHz, $li=0.92$, $ne=1.5 \times 10^{19} m^{-3}$, $Z_{eff}=2$, $B_t=5.3T$ and $N_{\parallel}=0.6$ at $R=6.2m$.

- [1] T. Maekawa, M. Uchida and H. Tanaka, Nucl. Fusion **58** (2018) 016037.
- [2] M. Bornatici, R. Cano, O. De Barbieri and F. Engelmann, Nucl. Fusion **23** (1983) 1153.
- [3] Y.R. Lin-Liu, V.S. Chan and R. Prater, Phys. Plasmas **10** (2003) 4064.
- [4] C.F.F. Karney and N.J. Fisch, Phys. Fluids, **29** (1986) 180.
- [5] S.M. Kaye and ITER Confinement Database Working Group Nucl. Fusion **37** (1997) 1303.